

Exergy analysis and optimization of a high temperature proton exchange membrane fuel cell using genetic algorithm



Maryam Haghighi ^{a,*}, Fatemeh Sharifhassan ^b

^a Department of Chemistry, Faculty of Physics & Chemistry, Alzahra University, P.O. Box 1993891176, Tehran, Iran

^b Department of Mechanic, Faculty of Engineering, Alzahra University, P.O. Box 1993891176, Tehran, Iran

ARTICLE INFO

Article history:

Received 20 November 2015

Received in revised form

20 July 2016

Accepted 30 July 2016

Available online 30 July 2016

Keywords:

Fuel cell

Exergy

Irreversibility

Exergy efficiency

Genetic algorithm

ABSTRACT

The exergy of a high temperature proton exchange membrane fuel cell has been studied and analyzed in this research. In the present work a genetic algorithm code was developed using MATLAB software to calculate and optimize work, exergy, exergy efficiency and thermodynamic irreversibility. Also, a membrane fuel cell was modeled and simulated. The polarization curve is in good agreement with experimental data. The results were studied for current density range=0.05 A/cm² to 1 A/cm², temperature range=393 K to 453 K, pressure range=1 atm to 3 atm and membrane thickness=0.016–0.02 cm. The optimum value of work was calculated 0.496 W/cm² that was obtained at current density of 1 A/cm², temperature=453 K, pressure=2.6 atm and membrane thickness=0.016 cm. The optimum value for irreversibility and exergy efficiency are 0.007 W/cm² and 0.46 at the same point. The optimum point of multi-objective function was obtained at current density 0.49363 A/cm², temperature 451.231 K, pressure 2.5 atm and membrane thickness 0.016 cm. At this optimum point work, irreversibility and exergy efficiency were calculated as 0.2767 W/cm², 0.1542 W/cm² and 0.3545 simultaneously.

© 2016 Published by Elsevier Ltd.

1. Introduction

Proton exchange membrane fuel cells (PEMFCs) are economic and environmentally friendly power generation that have been extensively used in recent years [1]. They are most promising candidate for electricity generation in automobiles and portable electronic devices [2–5]. In recent decade, the researches and development in fuel cell stacks accelerated due to energy crisis and environmental legislation [6,7]. Then, various experimental and theoretical models on PEMFCs have been developed [8–13]. Water and heat are by products of PEMFC [14]. The fuel cells can be integrated parallel in a stack which can be produces high range of power [15]. The PEMFC stacks receive more attention for high power generation, economic generation, easy start up and safe operating conditions [16]. The PEMFC performance is thus defined by many parameters, such as temperature, pressure, mass flow rate, H₂ and O₂ concentrations and relative humidity. Also, the geometric characteristics and electrolyte specifications are effective on fuel cell efficiency. Diffusivity of hydrogen and oxygen is a function of porosity, pore density and electrolyte material [17].

The heat is generated during a process in a fuel cell. The maximum useful work is in the equilibrium state with heat reservoir. In the equilibrium state between the system and environment, the exergy value is zero. The exergy shows the

* Corresponding author.

E-mail addresses: m.haghighi@alzahra.ac.ir, m.haghighi2010@gmail.com (M. Haghighi).

Nomenclature		ξ	Stoichiometric ratio, ratio of excess air and fuel
A	Membrane activity	λ_{mem}	Membrane water content
E	Exergy rate, kW	σ_{mem}	Membrane conductivity, $\text{U}^{-1} \text{cm}^{-1}$
E	Specific exergy, kJ/kg	η	Efficiency
F	Faradays constant, C mol^{-1}	α	Transfer coefficients
h	Enthalpy, J mol^{-1}		
I	Irreversibility, kW		
i	Current density, A cm^{-2}		
i_0	Exchange current density, A cm^{-2}		
n	Molar flow rate, kmol/s		
P	Pressure, atm		
R	Universal gas constant, $\text{mol}^{-1} \text{K}^{-1}$		
s	Specific entropy, $\text{J mol}^{-1} \text{K}^{-1}$		
T	Temperature, K		
t_{mem}	Membrane thickness, cm		
V	Cell potential, V		
W	Power, W		
x	Mole fraction		
<i>Greek letters</i>			
μ	Chemical potential, J mol^{-1}		
			<i>Subscripts</i>
		A	Anode
		Act	Activation
		C	Cathode
		Ch	Chemical
		Conc	Concentration
		FC	Fuel cell
		irrev	Irreversible
		in	Inlet
		mem	Membrane
		ohm	Ohmic
		out	Outlet
		pH	Physical
		rev	Reversible
		j	Species in the flow

reversibility of a process due to entropy increment [18–20]. The exergy is represented for a system and its environment and is not a property of the system. The enthalpy and entropy are measured for a system from a reference state. The internal energy of a system changes by changing different variables such as temperature, pressure and input mass flow rate [21]. The difference of internal energy of inputs and outputs and mechanical work of the system are the most important terms in exergy calculation [22]. Exergy value is the criteria for irreversibility of the system [23]. Maximum produced work of a fuel cell is the ideal work that is not available in a real system [24]. Also, exergy is represented the energy and work destruction of a cycle. The exergetic content was formulated in this research and the effect of variables on thermodynamic irreversibility was studied [25].

Exergy can be measured by experimental data. Experimental data are very limit due to the high test cost. Theoretical results are very helpful for predicting the results in a wide range of variables. The model usually prevents of many experiments which are demanded for analyzing the system. Then, the exergy analysis was studied to estimate the maximum useful work. In this research, exergy analysis is used to optimize the fuel cell operation.

2. Exergy analysis

The fuel cell consists of two electrodes anode and cathode and a porous polymeric electrolyte which was separated electrodes and the ion exchange was occurred. H_2 molecules diffuse via porous electrodes and protons produce at catalyst layer. Protons flow through the porous electrolyte and react with O^{2-} ions that produce H_2O and heat. Producing the electrical current in an external circuit is the main aim of a fuel cell. The electrolyte divides the fuel cell structure to two main sections and prevents from direct contact between hydrogen and oxygen [25–29].

Diffusion and reaction rate control the fuel cell performance. These phenomena should be compatible together. The operating condition, water content and reaction kinetics must be adjusted and optimized for a modular structure which is called fuel cell stack. Also, the exergy analysis of a fuel cell can be carried out to optimization. Also, two different approaches were proposed in different researches. Mechanistic models and empirical based approaches were used in various references [30]. The results of modeling can be linked to genetic algorithm code to find optimum. Then, momentum, heat transfer, mass, diffusion and electrochemical reactions should be modeled and solved together. These phenomena are very complex and are functions of different parameters. Mass diffusivity and catalyst characteristics are most important factors [31,32]. Optimization helps to adjust these parameters. Also, the exergy analysis is a key factor in improving the fuel cell design. In this research, the exergy was computed and optimized. To obtain exergy values and studying different parameters, a genetic algorithm was used.

In this research thermodynamic irreversibility, exergy efficiency and work were defined as objective functions. However this code was used for optimizing the operating condition, but can be used for other geometrical and process variables of fuel cell. In addition a multi-objective function with proper constraints were selected and optimized in this paper. The

results were graphically reported, described and also checked by other reported data.

2.1. Assumptions

In order to investigate the thermodynamic characteristics of a single high temperature proton exchange membrane fuel cell (HT-PEMFC) and its exergetic performance, some general assumptions are supposed as follows:

- HT-PEMFC operates under steady-state conditions.
- Hydrogen and oxygen flows are supposed incompressible and laminar.
- The theoretical amount of hydrogen is calculated based on the produced electrical current (using Faraday's constant). As well as, theoretical amount of oxygen will be reported based on calculated hydrogen and humidity value.
- All gases are ideal.
- Kinetic and potential exergies are neglected.
- Cell operating temperatures will be supposed 393 K, 413 K, 433 K and 453 K.
- Exergy analysis is carried out for 1 atm, 2 atm and 3 atm.
- Membrane thickness is 0.016 cm and 0.020 cm.
- Current density is selected in the range $0.01\text{--}1.0\text{ A.cm}^{-2}$ (with 0.05 A.cm^{-2} intervals).
- Dead state pressure is 1 atm and dead state temperature is 298.15 K.
- Heat loss ratio (r_{HL}) is 20% [22].
- Hydrogen and oxygen utilization ratios are 80% and 50%, respectively [26].
- Humidity of input hydrogen and oxygen will be neglected in exergy calculation. Also, the produced water is negligible due to its small value.
- The feed gases are humidified at 28 °C.

2.2. Modeling and simulation

Exergy analysis is a crucial concept in fuel cell cost assessment. It was pointed out that cost of produced electricity can be determined with regard to exergy value. In the other word, exergy is a proper criterion for economic evaluation of a system. Exergy is a function of enthalpy, entropy, work and irreversibility of a system. Details of exergy calculation and optimization have been developed in this research. Genetic algorithm is used to minimize exergy as a multi-objective function with defined constraints in this research.

Each molecule of hydrogen produces 2 electrons that are transferred via external circuit. The electrochemical reaction between hydrogen and oxygen at catalyst layer is shown by following equation:



Fig. 1. shows the exergy balance of a PEM fuel cell. The exergy of a fuel cell is wasted by heat, mass and work.

$$\sum \dot{E}x_{in} = \sum \dot{E}x_{out} + \dot{I} \quad (2)$$

$$\sum \dot{E}x_{mass,in} = \sum \dot{E}x_{mass,out} - \sum \dot{E}x_{heat} + \sum \dot{E}x_{work} + \dot{I}_{FC} \quad (3)$$

The exergy of feed and products are calculated by Eqs. (4) and (5):

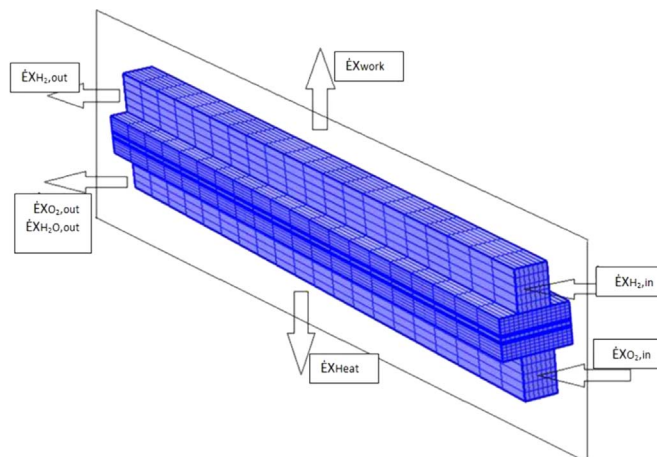


Fig. 1. Exergy balance of a PEMFC.

$$\sum \dot{E}x_{\text{mass.in}} = \dot{E}x_{\text{H}_2,\text{in}} + \dot{E}x_{\text{O}_2,\text{in}} = (\dot{n} \times ex)_{\text{H}_2,\text{in}} + (\dot{n} \times ex)_{\text{O}_2,\text{in}} \quad (4)$$

$$\sum \dot{E}x_{\text{mass.out}} = \dot{E}x_{\text{H}_2,\text{out}} + \dot{E}x_{\text{O}_2,\text{out}} + \dot{E}x_{\text{H}_2\text{O},\text{out}} = (\dot{n} \times ex)_{\text{H}_2,\text{out}} + (\dot{n} \times ex)_{\text{O}_2,\text{out}} + (\dot{n} \times ex)_{\text{H}_2\text{O},\text{out}} \quad (5)$$

Exergy can be defined with different terms such as physical exergy, kinetic exergy, chemical exergy and potential exergy. In this research only physical and chemical exergy are considered and kinetic and potential exergy are neglected [27,30]:

$$ex = ex^{PH} + ex^{CH} \quad (6)$$

$$ex^{PH} = (h - h_0) - T_0(s - s_0) \quad (7)$$

$$ex^{CH} = \sum_j x_j e_j^{CH} + RT_0 \sum x_j \ln x_j \quad (8)$$

Molar flow rates of hydrogen, oxygen and produced water are calculated by (Eqs. (9)–11):

$$\dot{n}_{\text{H}_2\text{O},\text{out}} = \frac{i}{2F} = \dot{n}_{\text{H}_2,\text{reacted}} = 2\dot{n}_{\text{O}_2,\text{reacted}} \quad (9)$$

$$\dot{n}_{\text{H}_2,\text{in}} = \dot{n}_{\text{H}_2,\text{reacted}} + \dot{n}_{\text{H}_2,\text{out}} \quad (10)$$

$$\dot{n}_{\text{O}_2,\text{in}} = \dot{n}_{\text{O}_2,\text{reacted}} + \dot{n}_{\text{O}_2,\text{out}} \quad (11)$$

The exergy waste due to the work is calculated by following equation:

$$\sum \dot{E}x_{\text{work}} = W_{FC} \quad (12)$$

The reversible cell voltage can be estimated by Nernst equation [31].

$$V_{\text{rev}} = 1.229 - 8.5 \times 10^{-4}(T_{FC} - 298.15) + 4.3085 \times 10^{-5} \times T_{FC} \left[\ln(p_{\text{H}_2}) + \frac{1}{2} \ln(p_{\text{O}_2}) \right] \quad (13)$$

Where the partial pressure of hydrogen and oxygen can be calculated by Eq. (14)–(17) [8].

$$x_{\text{H}_2\text{O},A} = \frac{P_{\text{sat}}}{P_A} \quad (14)$$

$$x_{\text{H}_2\text{O},C} = \frac{P_{\text{sat}}}{P_C} \quad (15)$$

$$p_{\text{H}_2} = \frac{1 - x_{\text{H}_2\text{O},A}}{1 + (x_A/2)(1 + \xi_A/\xi_A - 1)} \cdot P_A \quad (16)$$

$$p_{\text{O}_2} = \frac{1 - x_{\text{H}_2\text{O},C}}{1 + (x_C/2)(1 + \xi_C/\xi_C - 1)} \cdot P_C \quad (17)$$

Actual cell voltage is lower than of equilibrium state due to irreversibilities. Irreversibilities are classified in three groups: activation, ohmic and concentration losses. These losses are calculated by (Eqs. (18)–(20) [32–35]):

$$v_{\text{act}} = \left(\frac{\alpha_A + \alpha_C}{\alpha_A \alpha_C} \right) \frac{RT_{FC}}{nF} \ln \left(\frac{i}{i_0} \right) \quad (18)$$

$$v_{\text{ohm}} = i \times t_{\text{mem}} \times \left[(0.005139 \lambda_{\text{mem}} - 0.00326) \exp \left[1268 \left(\frac{1}{303} - \frac{1}{T_{FC}} \right) \right] \right]^{-1} \quad (19)$$

$$v_{\text{conc}} = i \left(\beta_1 \frac{i}{i_{\text{max}}} \right)^{\beta_2} \quad (20)$$

Where i_0 is exchange current density and can be determined at fuel cell operating temperature [36]:

$$i_0(T) = 1.08 \times 10^{-21} \times \exp(0.086 T_{FC}) \quad (21)$$

To calculate ohmic loss, membrane humidity shall be calculated [37]:

$$a = \frac{x_{\text{H}_2\text{O}} P}{P_{\text{sat}}} \quad (22)$$

$$\lambda_{\text{mem}} = \begin{cases} 0.043 + 17.81a - 39.85a^2 - 39.85a^3 & 0 < a \leq 1 \\ 14 + 1.4(a-1) & 1 < a \leq 3 \end{cases} \quad (23)$$

To calculate concentration loss, concentration overvoltage constants shall be defined. β_1 and β_2 are reported in different

researches [15]:

$$\beta_1 = \begin{cases} \text{if } \frac{P_{O_2}}{0.1173} + P_{sat} < 2atm \\ (7.16 \times 10^{-4} T_{FC} - 0.622) \left(\frac{P_{O_2}}{0.1173} + P_{sat} \right) + (-1.45 \times 10^{-3} T_{FC} + 1.68) \\ \text{else} \\ (8.66 \times 10^{-5} T_{FC} - 0.068) \left(\frac{P_{O_2}}{0.1173} + P_{sat} \right) + (-1.6 \times 10^{-4} T_{FC} + 0.54) \end{cases} \quad (24)$$

Then \dot{W}_{FC} (the consumed work of fuel cell) is calculated by Eq. (25).

$$\dot{W}_{FC} = V(i) \times i = i \times [V_{rev} - v_{act} - v_{ohm} - v_{conc}] \quad (25)$$

Finally, exergy due to heat loss is estimated by following equation:

$$\sum \dot{E}x_{heat} = r_{HL} \times \dot{Q}_{FC} \quad (26)$$

The \dot{Q}_{FC} is heat generation by fuel cell and can be calculated by Eq. (27).

$$\dot{Q}_{FC} = \dot{Q}_{rev} + \dot{Q}_{irrev} \quad (27)$$

Reversible heat is a function of cell operating temperature, current and entropy of reaction:

$$\dot{Q}_{rev} = (-T_{FC} \nabla S_T) \frac{i}{nF} \quad (28)$$

The entropy change and irreversible heat can be estimated as follows [38]:

$$\Delta S_T = -9967.35 \ln(T_{FC}) + 12414.83 \quad (29)$$

$$\dot{Q}_{irrev} = \left(-\frac{\Delta G_T}{nF} - V_{cell} \right) i \quad (30)$$

Where ΔG_T is the Gibbs free energy difference. As mentioned before, the amount of produced water in electrolyte is negligible. The enthalpy of water formation in vapor can be evaluated as:

$$\Delta H_{g,T} = \Delta H_f^l - \Delta H_T^{vap} \quad (31)$$

Where the amount of ΔH_f^l is reported 285,830 J [38].

$$\Delta H_T^{vap} = 3.6985 \times 10^{-4} T_{FC}^3 - 0.4834 T_{FC}^2 - 152.4258 T_{FC} + 68260.5789 \quad (32)$$

Eq. (33) shows the total heat which is generated by a PEMFC.

$$\dot{Q}_{FC} = \left(-\frac{\Delta H_{g,T}}{nF} - V_{cell} \right) i \quad (33)$$

Then, the thermodynamic irreversibility is rewritten as eq. (34):

$$\dot{I}_{FC} = \sum \dot{E}x_{heat} + \sum \dot{E}x_{mass,in} - \sum \dot{E}x_{mass,out} - \sum \dot{E}x_{work} \quad (34)$$

And, exergy efficiency of a PEM fuel cell is the ratio of work to exergy of input mass:

$$\eta_{exergy} = \frac{\dot{W}_{FC}}{\dot{E}x_{mass,in}} \quad (35)$$

3. Optimization, results and discussion

3.1. Model results

The model was simulated by Ansys Fluent V.15.0 software and the results were used in genetic algorithm developed code. The results of proposed model were compared to experimental results which were reported by Ubong data [17]. The polarization curves were plotted at $T=453$ K and $P=1$ atm. Fig. 2. shows the obtained data.

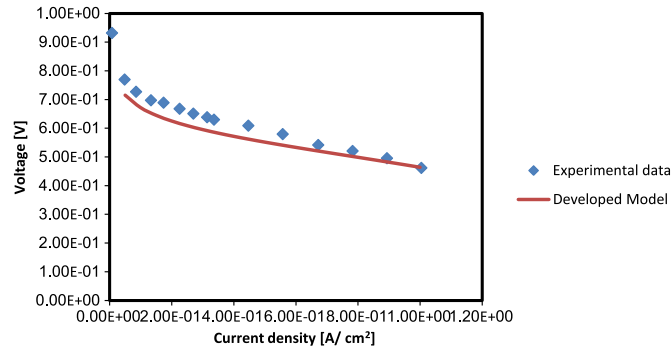


Fig. 2. Polarization curve data for developed model and experimental data [17].

Fig. 3. shows the variations of exergy efficiency with current density at constant membrane thickness of 0.016 cm and various operating pressure and temperature.

The results show that exergy efficiency decreases with increasing the current density. Also, exergy efficiency increases with increasing temperature. Raising the temperature increases mass exergy of feed and \dot{W}_{FC} simultaneously. Then $\dot{W}_{FC}/\dot{E}x_{mass,in}$ ratio increases. Pressure change has no significant effect on exergy efficiency. For instance at current density = 1 A/cm², T = 393 K and P = 1 atm, the exergy efficiency is 0.1529, for P = 2 atm is 0.2036 and for P = 3 atm is 0.1829. Fig. 3. represents that exergy efficiency values for P = 2 atm and P = 3 atm are similar.

Thermodynamic irreversibility is represented by input and output exergy and consumed work. This term is a criterion of irreversibility of a system. Fig. 4 shows the plot of thermodynamic irreversibility (\dot{I}_{FC}) versus current density at various operating pressures and temperatures. Membrane thickness of fuel cell is supposed 0.016 cm.

Fig. 4. represents that thermodynamic irreversibility increased with increasing the current density. Pressure and temperature rise have an inverse effect on thermodynamic irreversibility. The results confirm this effect. For instance the results show that at current density 1 A/cm², T = 393 K and P = 1 atm, thermodynamic irreversibility is equal to 0.9757 W/cm² and is reduced to 0.7298 at T = 453 K and P = 3 atm.

Fig. 5 illustrates the variation of exergy efficiency versus operating temperatures at different membrane thickness and current densities. The cell operating pressure is supposed 3 atm. It can be seen, exergy efficiency of a HT-PEMFC increases with temperature rise. Increasing the current density decreases exergy efficiency. Fig. 4. shows that thermodynamic irreversibility increased by increasing the current density. This is due to the increasing of $\dot{E}x_{mass,in}$. Therefore the ratio of work to input exergy decreased. In the other word, exergy efficiency decreases for higher current densities that it was shown in Fig. 5.

3.2. Optimization

The exergy function was modeled and the results were studied in previous section. The single-objective optimization of the system has been carried out to maximize the work and exergy efficiency of the system and to minimize thermodynamic irreversibility. Three single-objective optimization and a multi-objective optimization are studied in this research. Also, the exergy function is optimized by genetic algorithm. Decision variables are varied as mentioned in Table 1.

The main assumptions of single-objective optimization are listed in Table 2. Other assumptions were supposed as software defaults. The population, generation and iteration number were selected as follows.

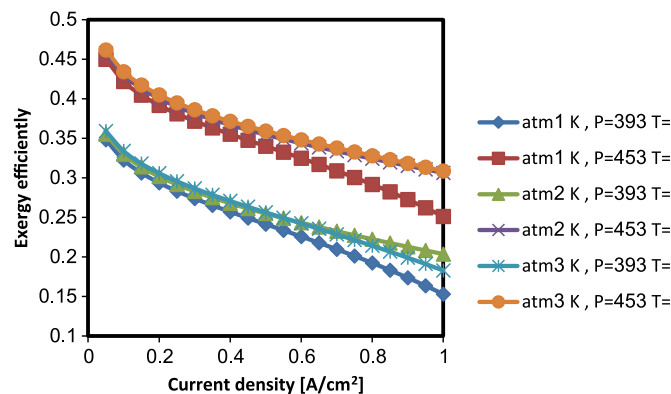


Fig. 3. Exergy efficiency versus current density in different operating temperature and pressure (membrane thickness is 0.016 cm).

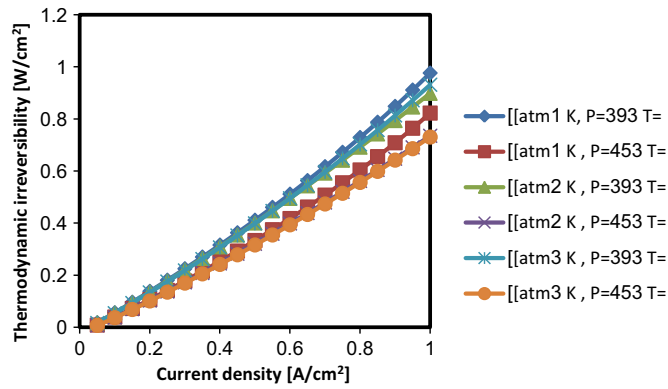


Fig. 4. Thermodynamic irreversibility versus current density at different operating temperature and pressure (membrane thickness is 0.016 cm).

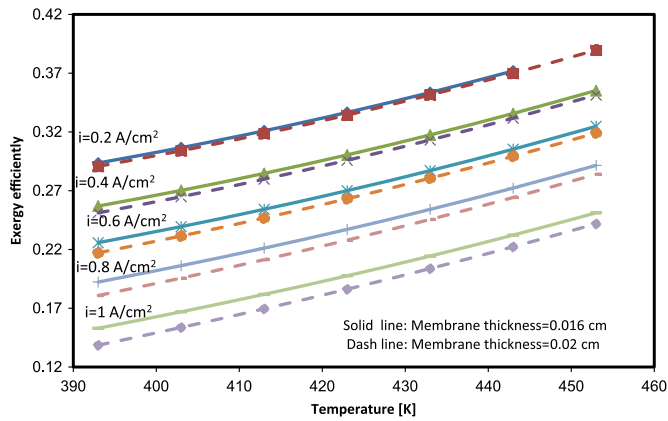


Fig. 5. Exergy efficiency versus temperature at different membrane thickness and current densities ($P=3$ atm).

Table 1

Decision variables.

Decision variables	Variation range
Current density [A/cm ²]	0.05–1
Temperature [K]	393–453
Pressure [atm]	1–3
Membrane thickness [cm]	0.016–0.02

Table 2

Assumptions in single-objective optimization (Genetic Algorithm).

The basic parameters of the genetic algorithm	Value
Population	100
Generation	200
Iteration	200

Other characteristics and results of the single-objective optimization of work have been summarized in Table 3. Current density, operating temperature, pressure and membrane thickness of three objective functions were supposed similar to

Table 3

The results and characteristics of single-objective optimization of work.

The objective function	Current density [A/cm ²]	Temperature [K]	Pressure [atm]	Membrane thickness [cm]	The objective function value [W/cm ²]
Work	1	453	2.6	0.016	0.496

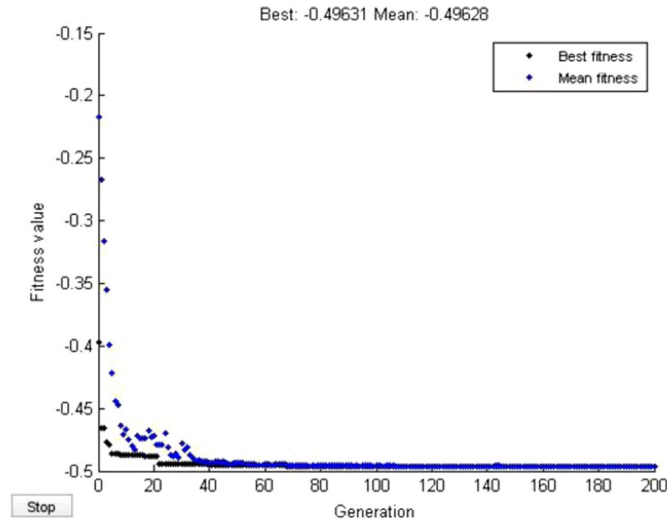


Fig. 6. Plot of a single-objective optimization of work.

each other.

Fig. 6 shows the plot of a single-objective optimization of work. The results show the best fitness was obtained at iteration 40.

Fig. 7 shows the diagram of a single-objective optimization of irreversibility. The optimization of irreversibility is achieved at generation no. 80.

Other theoretical results of the single-objective optimization of irreversibility have been presented in Table 4. The results show that irreversibility value at generation no. 200 is 0.007 W/cm² which is very low. In the other word the system is very efficient.

The exergy efficiency plays a key role in economic rating a fuel cell. Fig. 8. shows that the best fitness for exergy efficiency was obtained in lieu generation no. 100. The fitness value for this generation is –0.46. This value does not varied and remain constant. In the other word, increasing the generation number doesn't have not notable impact on accuracy.

The summary of optimization of results of exergy efficiency is presented in Table 5.

In the multi-objective optimization, optimum values for different functions are achieved simultaneously. The functions work, irreversibility and exergy efficiency only have an optimum value. Following objectives shall be optimized simultaneously:

$$f(1) = \text{Max}(\dot{W}_{FC}) f(2) = \text{Min}(\dot{I}_{FC}) f(3) = \text{Max}(\eta_{\text{exergy}})$$

The constraints for abovementioned objectives are as follows:

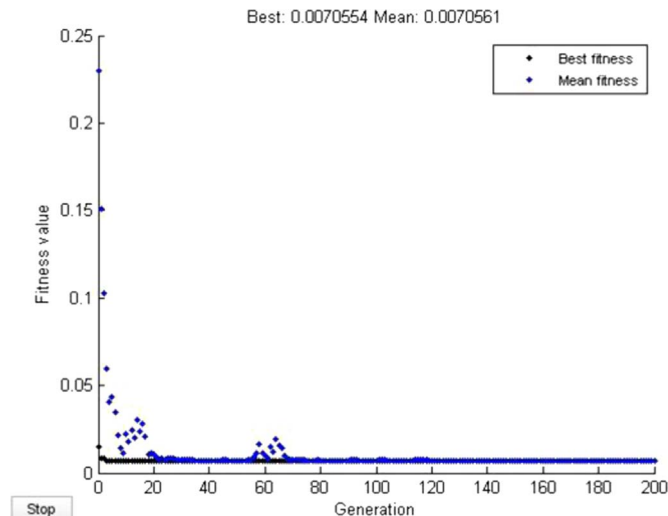


Fig. 7. Plot of a single-objective optimization of irreversibility.

Table 4
The results and characteristics of the single-objective optimization of irreversibility.

The objective function	Current density [A/cm ²]	Temperature [K]	Pressure [atm]	Membrane thickness [cm]	The objective function value [W/cm ²]
Irreversibility	0.05	453	3	0.016	0.007

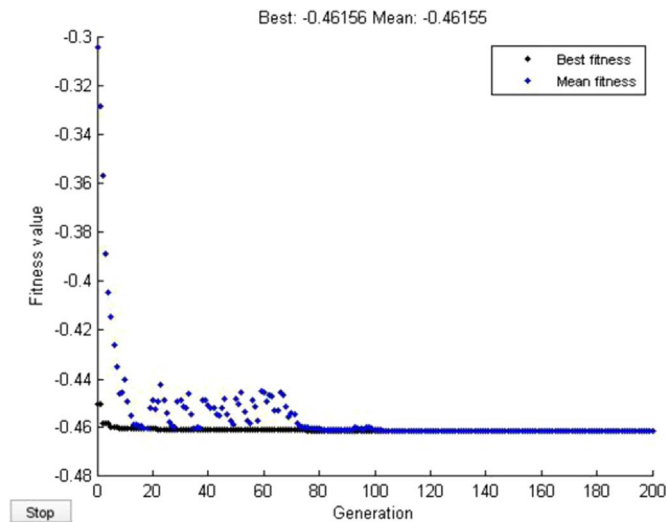


Fig. 8. Diagram of a single-objective optimization of exergy efficiency.

Table 5
The results of the single-objective optimization of exergy efficiency.

The objective function	Current density [A/cm ²]	Temperature [K]	Pressure [atm]	Membrane thickness [cm]	The objective function value
Exergy efficiency	0.05	453	3	0.016	0.46

$$0.05 \leq i = X(1) \leq 1 \left[\frac{A}{cm^2} \right] 393 \leq T = X(2) \leq 453 [K] 1 \leq P = X(3) \leq 3 [atm] 0.016 \leq t_{mem} = X(4) \leq 0.02 cm$$

The multi-objective function was solved with regards to defined constraints. Optimum point is a function of decision-making. This point is related to engineering data and the importance of each objective. In the other word, the aim is finding an ideal point. However each objective function shall be optimized separately but optimum point is determined together. All functions are satisfied at this point. LINMAP method is used to obtain dimensionless functions.

$$F_{ij}^n = \frac{F_{ij}}{\sqrt{\sum_{i=1}^m (F_{ij})^2}} \tag{36}$$

Where F denotes the objective, i is the index of each point on Pareto front graph, j is the index of each objective and m denotes the number of generation. Then the distance of each point on Pareto front from the ideal point is calculated by Eq. (37):

$$d_i = \sqrt{\sum_{j=1}^3 (F_{ij}^n - F_{ideal,j}^n)^2} \tag{37}$$

F_{ideal} shows ideal objective function. d_i represents deviation of objective function from ideal value. Minimum d indicates the final optimum solution [39]. The Pareto front of this multi-objective function was plotted for 60 populations and 150 iterations. Fig.9 shows this optimum point for all objective functions.

The optimum point is shown in Table 6. This point shows optimum work, irreversibility and exergy efficiency simultaneously.

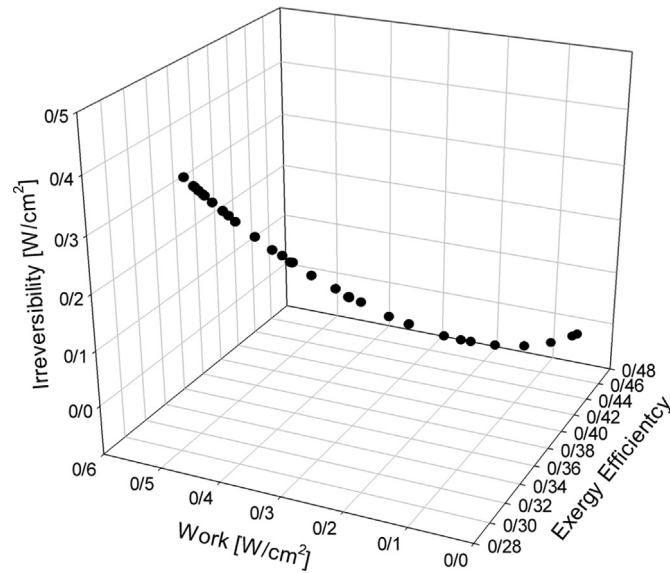


Fig. 9. Pareto front of defined multi-objective function.

Table 6
Optimum point.

Variable	Value
Current density [A/cm^2]	0.49363
Temperature [K]	451.2314
Pressure [atm]	2.5
Membrane thickness [cm]	0.016
Work [W/cm^2]	0.276733
Irreversibility [W/cm^2]	0.154178
Exergy efficiency	0.354485

4. Conclusion

In this research exergy analysis of a HT-PEMFC was considered and carried out under steady state condition. The cost optimization of the produced electrical power is dependent to energy waste. The exergy of a fuel cell is wasted by heat, work and output mass. The exergy balance of the fuel cell was modeled and simulated using Ansys Fluent V.15.0 software. Also, genetic algorithm was proposed for exergy analysis of a defined fuel cell by MATLAB software. The results were compared and validated by experimental data. The polarization curve was depicted at $T=453$ K and $P=1$ atm. The results show that there is good agreement between theoretical and experimental data. The exergy efficiency was plotted against the current density at different temperature and pressure (current density = 0.05 – 1 A/cm^2 and temperatures = 393 – 453 K). The exergy efficiency increases with temperature rising due to the increasing $\dot{W}_{FC}/\dot{E}x_{mass,in}$ function. Also, exergy efficiency is a function of membrane thickness but pressure has no important effect. The results show the thermodynamic irreversibility decreased with increasing temperature and pressure. The main objective of this work is optimization of fuel cell performance. Therefore, the exergy efficiency and work was described as single-objective functions and maximized. Also, thermodynamic irreversibility of the system should be minimized in order to optimization the system. The optimization code was developed using MATLAB software. Decision variables of these single-objective functions were selected as current density, temperature, pressure and membrane thickness. The best fitness for these single-objective functions were carried out at different generation number. Also, a multi-objective function was carried out and optimized by genetic algorithm method. The dimensionless functions were obtained by LINMAP method. The pareto front graph was plotted. The optimum point of multi objective functions was reported in Table 6. This point was obtained at Work = 0.276733 W/cm^2 , Irreversibility = 0.154178 W/cm^2 and Exergy efficiency = 0.354485 .

Acknowledgment

The authors thank the Alzahra University.

References

- [1] G. Zhang, S.G. Kandlikar, A critical review of cooling techniques in proton exchange membrane fuel cell stacks, *Int. J. Hydrog. Energy* 37 (3) (2012) 2412–2429.
- [2] S.-J. Cheng, J.-M. Miao, S.-J. Wu, Use of metamodeling optimal approach promotes the performance of proton exchange membrane fuel cell (PEMFC), *Appl. Energy* 105 (2013) 161–169.
- [3] B. Cheng, et al., A 10kW-scale distributed power plant of natural gas-proton exchange membrane fuel cell, *Chin. J. Chem. Eng.* 18 (6) (2010) 988–994.
- [4] J.-H. Wee, Applications of proton exchange membrane fuel cell systems, *Renew. Sustain. Energy Rev.* 11 (8) (2007) 1720–1738.
- [5] C. Damour, et al., A novel non-linear model-based control strategy to improve PEMFC water management—The flatness-based approach, *Int. J. Hydrog. Energy* (2015).
- [6] Y. Tang, et al., Experimental investigation on the dynamic performance of a hybrid PEM fuel cell/battery system for lightweight electric vehicle application, *Appl. Energy* 88 (1) (2011) 68–76.
- [7] P. Moçotéguy, B. Ludwig, N. Steiner, Influence of ageing on the dynamic behaviour and the electrochemical characteristics of a 500 We PEMFC stack, *Int. J. Hydrog. Energy* 39 (19) (2014) 10230–10244.
- [8] A. Rowe, X. Li, Mathematical modeling of proton exchange membrane fuel cells, *J. Power Sources* 102 (1) (2001) 82–96.
- [9] M.A. Sadiq Al-Baghdadi, Three-dimensional computational fluid dynamics model of a tubular-shaped PEM fuel cell, *Renew. Energy* 33 (6) (2008) 1334–1345.
- [10] Y. Wang, S. Basu, C.-Y. Wang, Modeling two-phase flow in PEM fuel cell channels, *J. Power Sources* 179 (2) (2008) 603–617.
- [11] L. You, H. Liu, A two-phase flow and transport model for PEM fuel cells, *J. Power Sources* 155 (2) (2006) 219–230.
- [12] J. Zhang, et al., High temperature PEM fuel cells, *J. Power Sources* 160 (2) (2006) 872–891.
- [13] H. Meng, A PEM fuel cell model for cold-start simulations, *J. Power Sources* 178 (1) (2008) 141–150.
- [14] Y. Wang, et al., A review of polymer electrolyte membrane fuel cells: technology, applications, and needs on fundamental research, *Appl. Energy* 88 (4) (2011) 981–1007.
- [15] Pukrushpan, J.T., A.G. Stefanopoulou, and H. Peng. Modeling and control for PEM fuel cell stack system. in: *Proceedings of the IEEE American Control Conference*, 2002.
- [16] Z.-D. Zhong, et al., A hybrid multi-variable experimental model for a PEMFC, *J. Power Sources* 164 (2) (2007) 746–751.
- [17] E. Ubong, Z. Shi, X. Wang, Three-dimensional modeling and experimental study of a high temperature PBI-based PEM fuel cell, *J. Electrochem. Soc.* 156 (10) (2009) B1276–B1282.
- [18] A.V. Akkaya, B. Sahin, H.H. Erdem, Exergetic performance coefficient analysis of a simple fuel cell system, *Int. J. Hydrog. Energy* 32 (17) (2007) 4600–4609.
- [19] R. Cownden, M. Nahon, M.A. Rosen, Exergy analysis of a fuel cell power system for transportation applications, *Exergy Int. J.* 1 (2) (2001) 112–121.
- [20] A. Kazim, Exergy analysis of a PEM fuel cell at variable operating conditions, *Energy Convers. Manag.* 45 (11) (2004) 1949–1961.
- [21] A. Ishihara, et al., Exergy analysis of polymer electrolyte fuel cell systems using methanol, *J. Power Sources* 126 (1) (2004) 34–40.
- [22] S. Mert, I. Dincer, Z. Ozelik, Performance investigation of a transportation PEM fuel cell system, *Int. J. Hydrog. Energy* 37 (1) (2012) 623–633.
- [23] S. Mert, I. Dincer, Z. Ozelik, Exergo economic analysis of a vehicular PEM fuel cell system, *J. Power Sources* 165 (1) (2007) 244–252.
- [24] T. Ratlamwala, M. Gadalla, I. Dincer, Thermodynamic analyses of an integrated PEMFC-TEARS-geothermal system for sustainable buildings, *Energy Build.* 44 (2012) 73–80.
- [25] M. Ay, A. Midilli, I. Dincer, Exergetic performance analysis of a PEM fuel cell, *Int. J. Energy Res.* 30 (5) (2006) 307–321.
- [26] W.-Y. Lee, et al., Empirical modeling of polymer electrolyte membrane fuel cell performance using artificial neural networks, *Int. J. Hydrog. Energy* 29 (9) (2004) 961–966.
- [27] T.J. Kotas, *The exergy method of thermal plant analysis*, Elsevier, 2013.
- [28] O.-J. Kwon, et al., A study of numerical analysis for PEMFC using a multiphysics program and statistical method, *Int. J. Hydrog. Energy* (2015).
- [29] F. Mathieu-Potvin, L. Gosselin, Optimal topology and distribution of catalyst in PEMFC, *Int. J. Hydrog. Energy* 39 (14) (2014) 7382–7401.
- [30] A. Bejan, M.J. Moran, *Thermal Design and Optimization*, John Wiley & Sons, 1996.
- [31] J.C. Amphlett, et al., Performance modeling of the Ballard Mark IV solid polymer electrolyte fuel cell I. Mechanistic model development, *J. Electrochem. Soc.* 142 (1) (1995) 1–8.
- [32] F. Barbir, T. Gomez, Efficiency and economics of proton exchange membrane (PEM) fuel cells, *Int. J. Hydrog. Energy* 21 (10) (1996) 891–901.
- [33] A.J. Bard, L.R. Faulkner, *Electrochemical Methods: Fundamentals and Applications*, Wiley, New York, 1980.
- [34] L. Guzzella, Control oriented modelling of fuel-cell based vehicles, in: *Proceedings of the NSF Workshop on Integration of Modelling and Control for Automotive System*, 1999.
- [35] M. Alberro, et al., Electronic modeling of a PEMFC with logarithmic amplifiers, *Int. J. Hydrog. Energy* 40 (9) (2015) 3708–3718.
- [36] T. Berning, D.M. Lu, N. Djilali, Three-dimensional computational analysis of transport phenomena in a PEM fuel cell, *J. Power Sources* 106 (1) (2002) 284–294.
- [37] T.E. Springer, T. Zawodzinski, S. Gottesfeld, Polymer electrolyte fuel cell model, *J. Electrochem. Soc.* 138 (8) (1991) 2334–2342.
- [38] E. Harikishan Reddy, S. Jayanti, Thermal management strategies for a 1 kWe stack of a high temperature proton exchange membrane fuel cell, *Appl. Therm. Eng.* 48 (2012) 465–475.
- [39] E. Khorasaninejad, H. Hajabdollahi, Thermo-economic and environmental optimization of solar assisted heat pump by using multi-objective particle swarm algorithm, *Energy* 72 (2014) 680–690.